

Synthesis, Biological Evaluation and Molecular Modeling of Pyrazole-Phthalazine Hybrid Derivatives Bearing 2-Aryloxy Quinoline Nucleus and their Computational Quantum Mechanical Modelling

PUJA SHARMA^{*✉}, RAJAT PATEL[✉], ROHIT R. KOSHTI[✉], AKSHAY VYAS[✉] and CHETAN B. SANGANI[✉]

Shri Maneklal M. Patel Institute of Sciences & Research, Kadi Sarva Vishwavidyalaya, Gandhinagar-382024, India

*Corresponding author: E-mail: madhav10722@gmail.com

Received: 25 June 2022;

Accepted: 18 September 2022;

Published online: 25 November 2022;

AJC-21042

In present work, the synthesis, characterization, antibacterial and anticancer activities of a novel series of 1*H*-pyrazolo[1,2-*b*]phthalazine-5,10-dione derivatives bearing 2-aryloxyquinoline nucleus (**6a-1**) is reported. *In vitro* antibacterial and anticancer activities against used strains and two cell lines A549 and HepG2 as well as enzyme inhibitory activities against EGFR and FabH were carried out. The most potent inhibitory activity against EGFR was displayed by compound **6l** and against FabH by compound **6i**. Docking studies showed that compound **6l** was bound to the active pocket of EGFR with hydrogen bond and π -H interaction with minimum binding energy and compound **6i** was bound to the active site of FabH with hydrogen bond and π -H interaction having minimum binding energy. DFT studies explained spatial arrangement as well as HOMO-LUMO to evaluate the plane angle. On the basis of their substitutions, these plane angles were then related with their activity against EGFR and FabH as well as antibacterial and anticancer activities.

Keywords: Pyrazole-Phthalazine hybrid, Antibacterial activity, Anticancer activity, Enzyme inhibitory activity, DFT.

INTRODUCTION

Due to the exceptional advantages of nitrogen-based heterocyclic compounds like ease of synthesis, lesser side effects, reduced drug resistance, better biocompatibility and higher bioavailability have proved to be a major step in drug discovery [1]. Heterocyclic compounds are mostly extracted from plants and animals and serve a vital role in the pharmaceutical industry [2]. Among the heterocyclic compounds, quinoline and its analogs play a noteworthy role in medicinal chemistry due to their exceptional biological and pharmacological activities [3,4]. Quinoline and its analogs are found to have antifungal, anticancer, antimalarial, antibacterial and anti-inflammatory properties [5]. Also, pyrazole and its derivatives have emerged as a potential class of heterocyclic compounds in the synthesis of new anticancer drugs due to their promising results for non-small cell lung cancer (A549) and liver cancer (HepG2) [6]. Similarly, phthalazine analogs due to their known pharmacological properties like anticancer, antidepressive, antimicrobial and antidiabetes as well as in the recent studies their use in the synthesis of anticancer drugs has emerged as a potentially new

area with promising scope in the development of novel anti-cancer drugs [7].

Studies on the EGFR-driven autocrine pathway indicated that the development and progression of cancer are largely governed by EGFR, a tyrosine-kinase enzyme found abundantly in the human epithelial cell membranes [8]. High levels of EGFR have been reported to be the major cause of a number of cancer types and are responsible for solid tumor growth [9]. The tyrosine kinases play a central role in cell growth and differentiation and also have a significant role in tumorigenesis which opens new avenues in medicinal intervention [10]. After ligand binding to EGFR, the receptor tyrosine kinase undergoes autophosphorylation, activating the downstream signal transduction pathways that ultimately result in EGFR inhibition and cancer cell death [11]. Thus, EGFRs are an important target for the designing of anticancer drugs [12]. Moreover, studies on the four generations of tyrosine kinase inhibitors indicate the increased resistance due to mutations in the kinase domain [13] of the first generation, low therapeutic window [14] offered by the second generation, low efficacy [15,16] in the third generation and the low efficacy of fourth-generation allosteric inhi-

bitors [17]. Due to these disadvantages, it is worthwhile to create novel scaffolds that can bind to both ATP and allosteric sites.

Another important area for designing new antibacterial drugs is type II fatty acid synthesis (FAS) in bacteria, which is essential for the survival of the cell and it also emphasizes the difference between bacterial and human fatty acid synthesis. The difference in the organization, enzyme structure and their specific roles makes for an attractive pathway for new drug discovery. Initiating the fatty acid elongation cycle and taking part in feedback control of the biosynthetic pathway *via* suppression of product accumulation, FabH, also known as β -ketoacyl-acyl carrier protein (ACP) synthase III, is an essential regulatory element in bacterial FAS. While Gram-positive and negative bacteria have an almost fixed sequence of FabH proteins in their structure, humans have no such significant homologous proteins. Furthermore, the Gram-positive and negative active site residues are almost identical, suggesting that FabH might serve as a viable target for the synthesis of novel antibacterial drugs with low toxicity, excellent selectivity and broad-spectrum antibacterial action [18-27].

Studies suggest that quinoline hybrids due to their low side effects and higher efficiency are a promising tool to develop new drugs and pharmacophores against cancer [28]. The MCR (multi-component reaction) approach is taken into consideration due to its simple process, varied structure, high yields and less waste generation to synthesize 1*H*-pyrazolo[1,2-*b*]phthalazine-5,10-dione [29,30]. This was done by the cyclocondensation of phthalhydrazide, aldehydes and malononitrile/ethyl cyanoacetate catalyzed by *p*-TSA [31], Et₃N₄ or [bmim]-OH [32]. However, 2-aryloxyquinolines-3-carbaldehyde has not been employed so far. Considering the pivotal biological role of recognition of 1*H*-pyrazolo[1,2-*b*]phthalazine-5,10-dione, a modification on the 1-position of 1*H*-pyrazolo[1,2-*b*]phthalazine-5,10-dione by 2-aryloxyquinolines-3-carbaldehyde is performed to check whether it may bring significant changes in the bioactivities of 1*H*-pyrazolo[1,2-*b*]phthalazine-5,10-dione or not. In the context of our interest in developing new antimicrobial agents *via* a combination of two therapeutically active moieties [15,16,33-37], herein, the synthesis of 1*H*-pyrazolo[1,2-*b*]phthalazine-5,10-dione (**6a-l**) derivatives by MCR approach is reported.

EXPERIMENTAL

The chemicals *viz.* acetanilide and its methyl and methoxy substituents, phenol and its fluoro derivatives, malononitrile, ethyl cyanoacetate, 2,3-dihydrophthalazine-1,4-dione and phosphorous oxychloride were purchased commercially and further purified by recrystallization and distillation, while the solvents (dimethyl formamide and ethanol) were of analytical grade. Thin-layer chromatography (TLC) on aluminium plates coated with silica gel 60 F₂₅₄, 0.25 mm thickness, Merck was used to monitor each step of the series. The XT4MP apparatus was used to find the melting points (uncorrected). ¹H NMR and ¹³C NMR spectra were recorded in DMSO-*d*₆ on a Bruker Avance 400 MHz spectrometer using DMSO as solvent. The CHN/S/O Elemental Analyzer 2400 Series II, Perkin-Elmer

was used for the elemental analysis (% C, H, N) and IR spectra were recorded on Perkin Elmer spectrum-GX spectrophotometer using KBr pellets. Mass spectra were scanned on a Thermo-fisher LCMS spectrometer.

Synthesis of 2-chloro-3-formylquinolines (1a-c): The synthesis of 2-chloro-3-formylquinolines (**1a-c**) was carried out using the Vilsmeier cyclization of substituted acetanilides. The Vilsmeier Haack reagent, chloromethyleneiminium salt, was prepared *in situ* by adding POCl₃ (12 mol) to DMF (3 mol) dropwise with continuous stirring using a magnetic stirrer and keeping the temperature between 0-5 °C. After complete addition, the resulting Vilsmeier Haack reagent was brought to room temperature and then the calculated quantity of substituted acetanilide (1 mol) was added and the mixture was refluxed in an RBF on a water bath for 6-7 h keeping the temperature at 90 °C. The resultant mixture was then brought at room temperature and poured into crushed ice where yellow precipitates of 2-chloro-3-formylquinolines (**1a-c**) separated out in good to moderate yield. The resulting precipitate was filtered, washed with water, dried and purified by recrystallization from ethyl acetate/acetonitrile with an overall yield of 62-69%.

It was observed that substitution at the *para* position affected the yield and the reaction time. Substitution of electron withdrawing groups at the *para* position increases the yield and reduces the reaction time. When there is no substitution (**1a**) on the *para*-position, the yield was 62% with higher reflux time, while in case of methoxy substitution on the *para*-position it gave higher yield of 69%, among all the synthesized molecule with lower reflux time.

Synthesis of 2-aryloxyquinoline-3-carbaldehyde (3a-f): 2-Chloro-3-formylquinolines (**1a-c**, 1 mol) and phenol (**2a-b**, 1 mol) were mixed and refluxed at 85 °C on a water bath using anhydrous K₂CO₃ as a base for 1.5 h. The reaction mixture was cooled and poured on crushed ice with continuous stirring followed by neutralization with 1.5 N HCl, which resulted in an excellent yield of 2-aryloxyquinoline-3-carbaldehyde (**3a-f**). The resulting precipitates were filtered, washed with water, dried and crystallized using ethanol. This reaction involved the nucleophilic substitution of the chloro group at C₂ in 2-chloro-3-formylquinolines (**1a-c**) with phenol (**2a-b**), where the yield was increased with a decrease in reaction time when an electron-withdrawing group like fluoro was substituted at the *para*-position of the phenol.

Synthesis of 3-amino-1-(2-(4-substituted phenoxy)-6-substituted quinolin-3-yl)-5,10-dioxo-5,10-dihydro-1*H*-pyrazolo[1,2-*b*]phthalazine-2-carbonitrile (6a-f) and ethyl 3-amino-1-(2-(4-substituted phenoxy)-6-substituted quinolin-3-yl)-5,10-dioxo-5,10-dihydro-1*H*-pyrazolo[1,2-*b*]phthalazine-2-carboxylate (6g-l): The synthesis of the target compounds **6a-f** and **6g-l** was carried out using the one-pot MCR approach. In RBF, 2-aryloxyquinoline-3-carbaldehyde (**3a-f**, 5 mmol) was added along with ethyl cyanoacetate or malononitrile (**4a-b**, 5 mmol) and 2,3-dihydro-1,4-phthalazine-dione (**5**, 5 mmol) with ethanol (10 mL) as solvent along with a catalytic amount of piperidine. The reaction mixture was heated under reflux for almost 4 h and it was monitored using thin-layer chromatography (TLC). After the completion of the

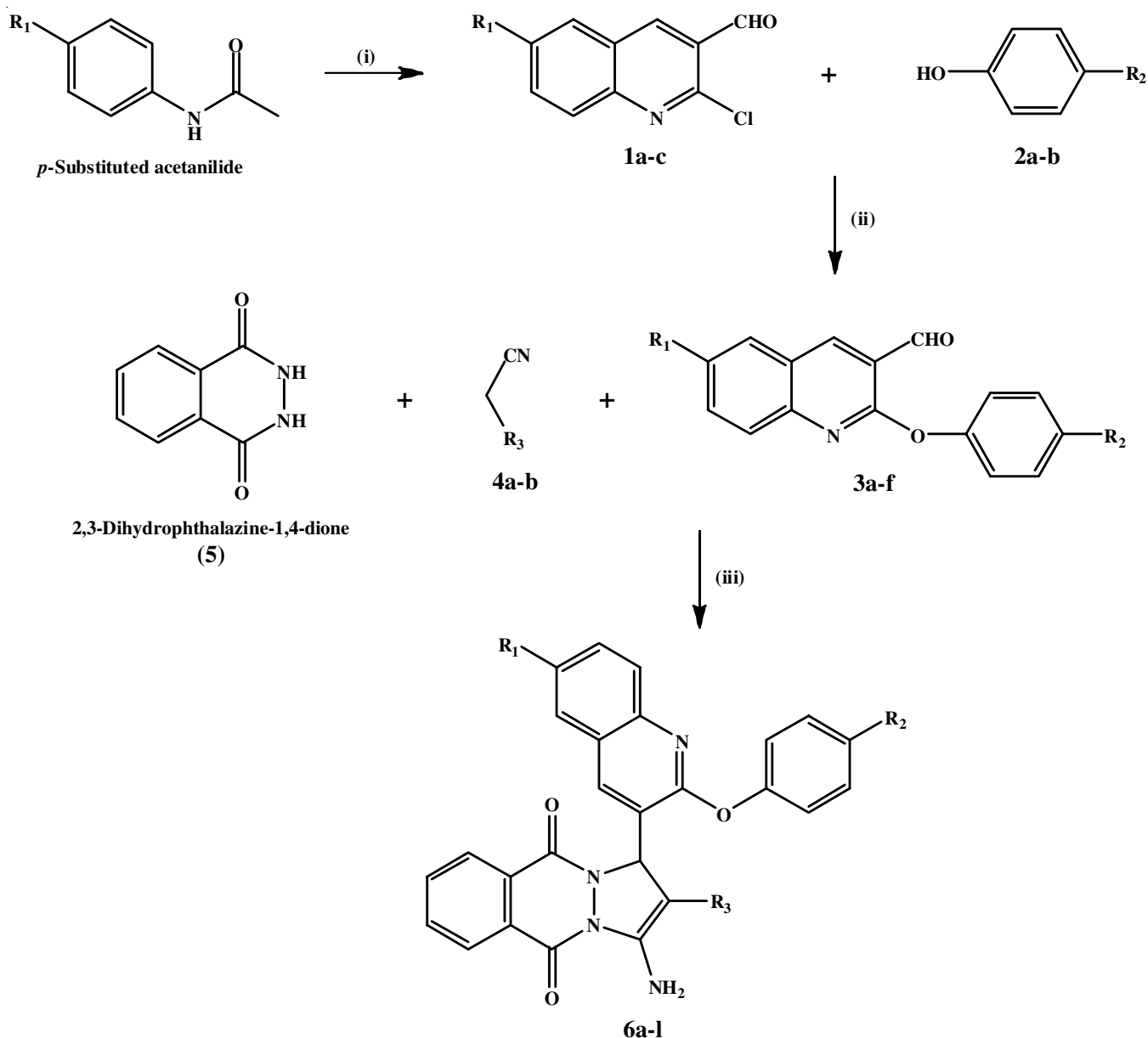
reaction, the solid separated was filtered and washed with ethanol to obtain the pure solid product.

This one-pot MCR approach was initially carried out *via* Knoevenagel condensation of **3a-f** and **4a-b** in the presence of a base to give an intermediate heterylidenenitrile which then proceeds *via* Micheal type addition of 2,3-dihydro-1,4-phthalazinedione (**5**) along with cyclization and tautomerization to give the target molecules **6a-f** and **6g-l**. The overall synthesis route is shown in **Scheme-I**.

3-Amino-5,10-dioxo-1-(2-phenoxyquinolin-3-yl)-5,10-dihydro-1H-pyrazolo[1,2-b]phthalazine-2-carbonitrile (6a): m.p.: 233-235 °C, yield: 89%. IR (KBr, ν_{\max} , cm^{-1}): 3390 & 3185 ($-\text{NH}_2$), 2200 ($-\text{C}\equiv\text{N}$), 1690 & 1685 ($-\text{C}=\text{O}$), 1605 ($-\text{C}=\text{N}-$), 1230 ($-\text{C}-\text{N}-$), 1205 ($-\text{C}-\text{O}-\text{C}-$), 1090 ($-\text{N}-\text{N}-$). $^1\text{H NMR}$ (400 MHz, $\text{DMSO}-d_6$) δ ppm: 6.56 (s, 1H, C_1H), 7.53-8.29

(m, 14H, Ar-H), 8.75 (s, 2H, $-\text{NH}_2$). $^{13}\text{C NMR}$ (400 MHz, $\text{DMSO}-d_6$) δ ppm: 59.40 (C_1), 61.38, 116.51 ($-\text{C}\equiv\text{N}$), 123.23, 124.34, 125.27, 127.34, 127.91, 128.10, 128.35, 128.68, 128.94, 129.43, 131.79, 132.21, 134.53, 135.31, 147.21, 154.31, 157.86, 160.01 (Ar-C), 156.85 ($-\text{C}=\text{O}$), 158.20 ($-\text{C}=\text{O}$). MS (m/z): 459.1 (M^+). Anal. calcd. (found) % for $\text{C}_{27}\text{H}_{17}\text{N}_5\text{O}_3$ ($m.w.$ 459.46 g/mol): C, 70.58 (70.42); H, 3.73 (3.92); N, 15.24 (15.47).

3-Amino-1-(6-methyl-2-phenoxyquinolin-3-yl)-5,10-dioxo-5,10-dihydro-1H-pyrazolo[1,2-b]phthalazine-2-carbonitrile (6b): m.p.: 251-253 °C, yield: 90%. IR (KBr, ν_{\max} , cm^{-1}): 3385 & 3190 ($-\text{NH}_2$), 2205 ($-\text{C}\equiv\text{N}$), 1680 & 1660 ($-\text{C}=\text{O}$), 1603 ($-\text{C}=\text{N}-$), 1232 ($-\text{C}-\text{N}-$), 1210 ($-\text{C}-\text{O}-\text{C}-$), 1093 ($-\text{N}-\text{N}-$). $^1\text{H NMR}$ (400 MHz, $\text{DMSO}-d_6$) δ ppm: 2.47 (s, 3H, $-\text{CH}_3$), 6.60 (s, 1H, C_1H), 7.40-8.35 (m, 13H, Ar-H), 8.61 (s, 2H, $-\text{NH}_2$). $^{13}\text{C NMR}$ (400 MHz, $\text{DMSO}-d_6$) δ ppm: 21.56 (Ar- CH_3),



Scheme-I: Synthesis of compounds **6a-l**, Reagents and conditions: (i) DMF, POCl_3 , reflux, (ii) DMF, K_2CO_3 , reflux, (iii) EtOH, piperidine, reflux

60.16 (C₁), 62.15, 117.05 (-C≡N), 123.01, 124.84, 125.51, 126.23, 126.36, 127.10, 127.46, 127.86, 128.53, 128.80, 131.14, 132.14, 133.74, 135.15, 145.82, 154.95, 158.03, 159.95 (Ar-C), 157.05 (-C=O), 158.43 (-C=O). MS (*m/z*): 473.1 (M⁺). Anal. calcd. (found) % for C₂₈H₁₉N₅O₃ (473.48 g/mol): C, 71.03 (69.75); H, 4.04 (3.89); N, 14.79 (14.48).

3-Amino-1-(6-methoxy-2-phenoxyquinolin-3-yl)-5,10-dioxo-5,10-dihydro-1H-pyrazolo[1,2-*b*]phthalazine-2-carbonitrile (6c): m.p.: 259-261 °C, yield: 86%. IR (KBr, ν_{\max} , cm⁻¹): 3385 & 3200 (-NH₂), 2195 (-C≡N), 1680 & 1670 (-C=O), 1601 (-C=N-), 1235 (-C-N-), 1215 (-C-O-C-), 1090 (-N-N-). ¹H NMR (400 MHz, DMSO-*d*₆) δ ppm: 3.82 (s, 3H, -OCH₃), 6.45 (s, 1H, C₁H), 7.62-8.34 (m, 13H, Ar-H), 8.46 (s, 2H, -NH₂). ¹³C NMR (400 MHz, DMSO-*d*₆) δ ppm: 55.92 (Ar-OCH₃), 59.20 (C₁), 61.94, 106.14, 117.26 (-C≡N), 123.35, 124.68, 125.12, 126.03, 126.90, 127.38, 127.93, 128.15, 129.40, 131.42, 133.65, 134.54, 135.10, 147.18, 154.23, 157.22, 159.38 (Ar-C), 157.18 (-C=O), 158.35 (-C=O). MS (*m/z*): 489.1 (M⁺). Anal. calcd. (found) % for C₂₈H₁₉N₅O₄ (489.48 g/mol): C, 68.71 (68.93); H, 3.91 (4.15); N, 14.31 (14.17).

3-Amino-1-(2-(4-fluorophenoxy) quinolin-3-yl)-5,10-dioxo-5,10-dihydro-1H-pyrazolo[1,2-*b*]phthalazine-2-carbonitrile (6d): m.p.: 213-215 °C, yield: 87%. IR (KBr, ν_{\max} , cm⁻¹): 3395 & 3225 (-NH₂), 2200 (-C≡N), 1685 & 1665 (-C=O), 1605 (-C=N-), 1350 (-C-F), 1232 (-C-N-), 1190 (-C-O-C-), 1085 (-N-N-). ¹H NMR (400 MHz, DMSO-*d*₆) δ ppm: 6.58 (s, 1H, C₁H), 7.56-8.67 (m, 13H, Ar-H), 8.85 (s, 2H, -NH₂). ¹³C NMR (400 MHz, DMSO-*d*₆) δ ppm: 58.92 (C₁), 61.11, 116.99 (-C≡N), 124.11, 125.65, 126.83, 127.35, 127.88, 128.29, 128.89, 129.44, 129.65, 131.64, 132.76, 134.18, 134.90, 147.71, 154.23, 157.33, 158.43, 160.27 (Ar-C), 157.67 (-C=O), 158.40 (-C=O). MS (*m/z*): 477.1 (M⁺). Anal. calcd. (found) % for C₂₇H₁₆N₅O₃F (477.45 g/mol): C, 67.92 (68.15); H, 3.38 (3.56); N, 14.67 (14.82).

3-Amino-1-(2-(4-fluorophenoxy)-6-methylquinolin-3-yl)-5,10-dioxo-5,10-dihydro-1H-pyrazolo[1,2-*b*]phthalazine-2-carbonitrile (6e): m.p.: 240-242 °C, yield: 90%. IR (KBr, ν_{\max} , cm⁻¹): 3390 & 3205 (-NH₂), 2210 (-C≡N), 1675 & 1665 (-C=O), 1604 (-C=N-), 1355 (-C-F), 1236 (-C-N-), 1200 (-C-O-C-), 1089 (-N-N-). ¹H NMR (400 MHz, DMSO-*d*₆) δ ppm: 2.44 (s, 3H, -CH₃), 6.62 (s, 1H, C₁H), 7.23-8.57 (m, 12H, Ar-H), 8.79 (s, 2H, -NH₂). ¹³C NMR (400 MHz, DMSO-*d*₆) δ ppm: 21.45 (Ar-CH₃), 60.05 (C₁), 61.45, 116.31 (-C≡N), 124.27, 125.40, 126.88, 127.20, 127.80, 128.15, 128.74, 129.22, 129.79, 130.15, 133.18, 134.35, 135.59, 146.88, 154.34, 157.92, 158.36, 159.73 (Ar-C), 157.90 (-C=O), 158.90 (-C=O). MS (*m/z*): 491.1 (M⁺). Anal. calcd. for C₂₈H₁₈N₅O₃F (491.47 g/mol): C, 68.43 (68.20); H, 3.69 (3.38); N, 14.25 (14.40).

3-Amino-1-(2-(4-fluorophenoxy)-6-methoxyquinolin-3-yl)-5,10-dioxo-5,10-dihydro-1H-pyrazolo[1,2-*b*]phthalazine-2-carbonitrile (6f): m.p.: 280-282 °C, yield: 82%. IR (KBr, ν_{\max} , cm⁻¹): 3390 & 3195 (-NH₂), 2200 (-C≡N), 1690 & 1675 (-C=O), 1606 (-C=N-), 1352 (-C-F), 1234 (-C-N-), 1195 (-C-O-C-), 1090 (-N-N-). ¹H NMR (400 MHz, DMSO-*d*₆) δ ppm: 3.86 (s, 3H, -OCH₃), δ 6.54 (s, 1H, C₁H), 7.80-8.48 (m, 12H, Ar-H), 8.77 (s, 2H, -NH₂). ¹³C NMR (400 MHz, DMSO-*d*₆) δ ppm: 55.94 (Ar-OCH₃), 60.20 (C₁), 61.69, 106.24, 116.56

(-C≡N), 124.21, 127.22, 127.83, 128.45, 128.85, 129.07, 129.78, 130.28, 132.83, 133.99, 134.85, 135.36, 147.49, 154.50, 157.03, 158.12, 160.13 (Ar-C), 156.98 (-C=O), 158.68 (-C=O). MS (*m/z*): 507.1 (M⁺). Anal. calcd. (found) % for C₂₈H₁₈N₅O₄F (*m.w.* 507.47 g/mol): C, 66.27 (66.61); H, 3.58 (3.24); N, 13.80 (14.11).

Ethyl 3-amino-5,10-dioxo-1-(2-phenoxyquinolin-3-yl)-5,10-dihydro-1H-pyrazolo[1,2-*b*]phthalazine-2-carboxylate (6g): m.p.: 221-223 °C, yield: 87%. IR (KBr, ν_{\max} , cm⁻¹): 3460 & 3335 (-NH₂), 1705 (-COO-), 1675 & 1655 (-C=O), 1602 (-C=N-), 1230 (-C-N-), 1190 (-C-O-C-), 1096 (-N-N-). ¹H NMR (400 MHz, DMSO-*d*₆) δ ppm: 1.02 (t, 3H, -CH₃), 3.99 (q, 2H, -OCH₂-), 6.52 (s, 1H, C₁H), 7.68-8.37 (m, 14H, Ar-H), 8.70 (s, 2H, -NH₂). ¹³C NMR (400 MHz, DMSO-*d*₆) δ ppm: 14.50 (-CH₃), 58.99 (C₁), 63.85 (-OCH₂), 82.06, 123.82, 124.28, 125.80, 126.75, 127.12, 127.54, 127.80, 127.95, 128.14, 129.53, 131.41, 132.24, 134.38, 135.94, 146.52, 154.94, 157.32, 159.19 (Ar-C), 156.89 (-C=O), 158.50 (-C=O), 164.40 (-COOEt). MS (*m/z*): 506.1 (M⁺). Anal. calcd. (found) % for C₂₉H₂₂N₄O₅ (506.51 g/mol): C, 68.77 (68.98); H, 4.38 (4.52); N, 11.06 (11.21).

Ethyl 3-amino-1-(6-methyl-2-phenoxyquinolin-3-yl)-5,10-dioxo-5,10-dihydro-1H-pyrazolo[1,2-*b*]phthalazine-2-carboxylate (6h): m.p.: 255-257 °C, yield: 82%. IR (KBr, ν_{\max} , cm⁻¹): 3455 & 3325 (-NH₂), 1695 (-COO-), 1670 & 1650 (-C=O), 1605 (-C=N-), 1233 (-C-N-), 1205 (-C-O-C-), 1090 (-N-N-). ¹H NMR (400 MHz, DMSO-*d*₆) δ ppm: 1.0 (t, 3H, -CH₃), 2.52 (s, 3H, Ar-CH₃), 4.01 (q, 2H, -OCH₂), 6.42 (s, 1H, C₁H), 7.30-8.37 (m, 13H, Ar-H), 8.47 (s, 2H, -NH₂). ¹³C NMR (400 MHz, DMSO-*d*₆) δ ppm: 14.30 (-CH₃), 21.62 (Ar-CH₃), 59.85 (C₁), 63.49 (-OCH₂), 82.45 (C₂), 123.82, 124.31, 124.95, 126.27, 127.20, 127.54, 127.68, 128.92, 129.13, 129.46, 130.29, 132.43, 134.26, 135.21, 145.74, 153.84, 156.55, 158.20 (Ar-C), 157.26 (-C=O), 158.14 (-C=O), 164.15 (-COOEt). MS (*m/z*): 520.1 (M⁺). Anal. calcd. (found) % for C₃₀H₂₄N₄O₅ (*m.w.* 520.54 g/mol): C, 69.22 (69.45); H, 4.65 (4.87); N, 10.76 (10.47).

Ethyl 3-amino-1-(6-methoxy-2-phenoxyquinolin-3-yl)-5,10-dioxo-5,10-dihydro-1H-pyrazolo[1,2-*b*]phthalazine-2-carboxylate (6i): m.p.: 244-246 °C, yield: 80%. IR (KBr, ν_{\max} , cm⁻¹): 3460 & 3300 (-NH₂), 1700 (-COO-), 1680 & 1660 (-C=O), 1607 (-C=N-), 1230 (-C-N-), 1210 (-C-O-C-), 1095 (-N-N-). ¹H NMR (400 MHz, DMSO-*d*₆) δ ppm: 0.98, (t, 3H, -CH₃), 3.82 (s, 3H, -OCH₃), 3.98 (q, 2H, -OCH₂), 6.56 (s, 1H, C₁H), 7.75-8.35 (m, 13H, Ar-H), 8.40 (s, 2H, -NH₂). ¹³C NMR (400 MHz, DMSO-*d*₆) δ ppm: 14.31 (-CH₃), 55.90 (Ar-OCH₃), 59.56 (C₁), 63.77 (-OCH₂), 82.13 (C₂), 106.10, 123.54, 124.14, 124.82, 126.05, 127.10, 127.59, 128.25, 128.58, 130.28, 131.37, 132.46, 133.89, 135.25, 145.84, 154.15, 157.14, 160.47 (Ar-C), 157.11 (-C=O), 158.66 (-C=O), 164.29 (-COOEt). MS (*m/z*): 536.1 (M⁺). Anal. calcd. (found) % for C₃₀H₂₄N₄O₆ (536.53 g/mol): C, 67.16 (67.39); H, 4.51 (4.86); N, 10.44 (10.73).

Ethyl 3-amino-1-(2-(4-fluorophenoxy) quinolin-3-yl)-5,10-dioxo-5,10-dihydro-1H-pyrazolo[1,2-*b*]phthalazine-2-carboxylate (6j): m.p.: 227-229 °C, Yield: 81%. IR (KBr, ν_{\max} , cm⁻¹): 3400 & 3330 (-NH₂), 1710 (-COO-), 1680 & 1660 (-C=O), 1607 (-C=N-), 1355 (-C-F), 1233 (-C-N-), 1215 (-C-O-C-), 1089 (-N-N-). ¹H NMR (400 MHz, DMSO-*d*₆) δ ppm: 1.08 (t, 3H, -CH₃), 3.95 (q, 2H, -OCH₂-), 6.47 (s, 1H, C₁H), 7.48-8.34 (m, 13H, Ar-H), 8.56 (s, 2H, -NH₂). ¹³C NMR (400 MHz, DMSO-

d_6) δ ppm: 14.20 (-CH₃), 59.45 (C₁), 64.01 (-OCH₂), 81.95 (C₂), 123.12, 124.43, 126.83, 127.21, 127.42, 127.83, 128.43, 129.25, 129.48, 129.80, 131.24, 134.19, 135.72, 145.74, 153.81, 156.92, 158.43, 160.17 (Ar-C), 156.84 (-C=O), 158.78 (-C=O), 164.25 (-COOEt). MS (m/z): 524.1 (M⁺). Anal. calcd. (found) % for C₂₉H₂₁N₄O₅F (524.50 g/mol): C, 66.41 (66.67); H, 4.04 (3.86); N, 10.68 (10.87).

Ethyl 3-amino-1-(2-(4-fluorophenoxy)-6-methylquinolin-3-yl)-5,10-dioxo-5,10-dihydro-1H-pyrazolo[1,2-b]phthalazine-2-carboxylate (6k): m.p.: 272-274 °C, yield: 74%. IR (KBr, ν_{\max} , cm⁻¹): 3415 & 3340 (-NH₂), 1705 (-COO-), 1680 & 1670 (-C=O), 1605 (-C=N-), 1350 (-C-F), 1235 (-C-N-), 1215 (-C-O-C-), 1085 (-N-N-). ¹H NMR (400 MHz, DMSO- d_6) δ ppm: 0.96 (t, 3H, -CH₃), 2.46 (s, 3H, Ar-CH₃), 4.03 (q, 2H, -OCH₂-), 6.51 (s, 1H, C₁H), 7.39-8.58 (m, 12H, Ar-H), 8.64 (s, 2H, -NH₂). ¹³C NMR (400 MHz, DMSO- d_6) δ ppm: 14.54 (-CH₃), 21.40 (Ar-CH₃), 59.76 (C₁), 63.50 (-OCH₂), 82.26 (C₂), 124.76, 127.31, 127.58, 128.14, 128.69, 129.13, 129.67, 132.24, 133.33, 134.84, 135.15, 136.75, 145.81, 148.74, 155.34, 157.00, 158.32, 160.10 (Ar-C), 156.20 (-C=O), 158.41 (-C=O), 164.62 (-COOEt). MS (m/z): 538.2 (M⁺). Anal. calcd. (found) % for C₃₀H₂₃N₄O₅F (538.53 g/mol): C, 66.91 (66.75); H, 4.30 (4.47); N, 10.40 (10.24).

Ethyl 3-amino-1-(2-(4-fluorophenoxy)-6-methoxyquinolin-3-yl)-5,10-dioxo-5,10-dihydro-1H-pyrazolo[1,2-b]phthalazine-2-carboxylate (6l): m.p.: 248-250 °C, yield: 78%. IR (KBr, ν_{\max} , cm⁻¹): 3390 & 3280 (-NH₂), 1700(-COO-), 1680 & 1665 (-C=O), 1602 (-C=N-), 1353 (-C-F), 1232 (-C-N-), 1205 (-C-O-C-), 1091 (-N-N-). ¹H NMR (400 MHz, DMSO- d_6) δ ppm: 1.07 (t, 3H, -CH₃), 3.80 (s, 3H, -OCH₃), 4.00 (q, 2H, -OCH₂-), 6.50 (s, 1H, C₁H), 7.71-8.61 (m, 12H, Ar-H), 8.69 (s, 2H, -NH₂). ¹³C NMR (400 MHz, DMSO- d_6) δ ppm: 14.49 (-CH₃), 55.85 (Ar-OCH₃), 60.11 (C₁), 63.30 (-OCH₂), 82.37 (C₂), 106.37, 124.13, 127.13, 127.60, 128.34, 128.89, 129.27, 129.85, 130.23, 131.34, 133.64, 134.16, 135.42, 145.64, 152.62, 156.79, 158.22, 159.18 (Ar-C), 155.90 (-C=O), 158.20 (-C=O), 164.36 (-COOEt). MS (m/z): 554.2 (M⁺). Anal. calcd. (found) % for C₃₀H₂₃N₄O₆F (554.53 g/mol): C, 64.98 (65.12); H, 4.18 (4.30); N, 10.10 (10.26).

MTT base colorimetric assay: The antiproliferative activities of synthesized compounds **6a-l** were analyzed by using a standard MTT based colorimetric assay. For this, in 96-well microtiter plates, (Costar) cell lines were seeded at a density of 7000 cells per well. Rapidly growing cells were brought to the indicated compounds at final concentrations ranging from 0.1 to 40 mg/mL after 24 h. The cell survival was determined after 48 h by the incorporation of an MTT solution (20 μ L of 5 mg/mL MTT in PBS). After 6 h, 100 μ L of 10% SDS in 0.01 N HCl was added, after which plates were incubated at 37 °C for 4 h. A LX300 Epson Diagnostic microplate reader was used to measure optical absorbance at 570 nm. The ratios of the survival cell were pointed in percentages with respect to untreated cells. The IC₅₀ values were carried out from replicates of 6 wells by results of at least two independent experiments.

EGFR inhibitory assay: Cloning of a 1.6 kb cDNA was performed to study the EGFR inhibitory assay. cDNA was

encoded for the EGFR cytoplasmic domain (EGFR-CD, amino acids 645-1186) into baculoviral expression vectors pFAST-BacHTc (Huakang, China) and pBlueBacHis2B, separately. Determination of protein expression was analyzed for three days by means of a sequence that encodes (His)₆ and found to be located at the 50 upstream to the EGFR sequences. Protein expressions were also checked by infecting Sf-9 cells for three days. The Sf-9 cell pellets were solubilized at 0 °C in a buffer solution at pH 7.4 having 50 mM HEPES, 10 mM NaCl, 1% solution of Triton, 1 \times 10⁻⁵ M ammonium molybdate solution, 1 \times 10⁻⁴ M sodium vanadate solution, 10 ppb solution of aprotinin, 10 ppb solution of leupeptin, 10 ppb solution of pep-statin and 16 ppb solution of benzamidine HCl salt for 20 min, which was further treated with centrifugation for another 20 min. The extracted crude material was, then passed through an equilibrated Ni-NTA super flow packed column to remove non-specifically bound material. The crude material was washed with 1 \times 10⁻² M and 0.1 M solution of imidazole, respectively. Proteins tagged with histidine were eluted using 0.25 M and 0.50 M imidazole solution. The eluted proteins were then dialyzed against 0.05 M NaCl solution, 0.02 M HEPES, 10% glycerol and 1 ppb each of aprotinin, leupeptin and pep-statin for 2 h. This whole procedure for the purification of crude was carried out at 4 °C [38].

EGFR kinase assay was used to confirm the level of autophosphorylation based on DELFIA/time-resolved fluorometry. The synthesized compounds **6a-l** were dissolved in 100% DMSO. This solution was diluted to the appropriate concentrations with 25 mM HEPES at pH 7.4. This was done by incubating 10 μ L compound in each well with 10 μ L (5 ng for EGFR) recombinant enzyme (1:80 dilution in 100 mM HEPES) for 10 min at room temperature. This was followed by the addition of 20 μ L of 0.1 mM ATP-50 mM MgCl₂ and 10 μ L of 5 \times buffer (containing 20 mM HEPES, 2 mM MnCl₂, 100 μ M Na₃VO₄ and 1 mM DTT) for 1 h. Negative and positive controls were included in each plate by incubation of the enzyme with or without ATP-MgCl₂. All further process of FaBH inhibitory assay were performed as per reported method [39].

FaBH inhibitory assay: FaBH purification and activity assay was carried out on the individual cloning of full-length *E. coli* acyl carrier protein (ACP), acyl carrier protein synthase (ACPS) and b-ketoacyl-ACP synthase III (FabH) into pET expression vectors by assigning His-tag (ACP, ACPS in pET19; FabH in pET28) as N-terminal. All further process of FaBH inhibitory assay were performed as per reported method [39].

MICs study of antibacterial activity: The antibacterial activities of synthesis compounds **6a-l** were against *B. subtilis*, *S. aureus*, *E. coli* and *P. aeruginosa* using Mueller-Hinton medium. The MICs (minimum inhibitory concentrations) of the test compounds by colorimetric method using the dye MTT. The MICs study of antibacterial activity assay were performed as per reported method [40].

Docking study: Auto-Dock software package (version 4.0) as implemented through the graphical user interface Auto-Dock Tool Kit (ADT 1.4.6) [38] was used to carry out the Molecular docking for all synthesized compounds **6a-l** into the three-dimensional EGFR complex structure (PDB code:

1M17) as well as into the three-dimensional structure of *E. coli* FabH (PDB code: 1HNJ).

RESULTS AND DISCUSSION

A new series of 1*H*-pyrazolo[1,2-*b*]phthalazine-5,10-dione derivatives having 2-aryloxyquinoline moiety has been synthesized by base catalyzed one-pot multi-component reaction in good yield. The stretching or bending of the substituted and linkage functional groups is confirmed by the infrared spectra for all the compounds. The medium intensity asymmetric and symmetric stretching bands of the primary amine (-NH₂) were observed in regions of 3460-3385 and 3340-3185 cm⁻¹ for all compounds. The cyanide group (-C≡N) shows a weak stretching band in the region of 2210-2195 cm⁻¹ for compounds **6a-f**. The stretching vibration of carbonyl ester (-COO-) appeared in the region of 1710-1695 cm⁻¹ for compounds **6g-l**. The strong stretching between carbon and oxygen of the carbonyl (-C=O-) group containing phthalazine ring appeared in the regions of 1690-1670 and 1675-1650 cm⁻¹, while the carbon and nitrogen medium stretching of C=N containing quinoline ring appeared in the region of 1607-1601 cm⁻¹ for all compounds. The strong carbon and fluorine stretching of C-F containing phenoxy ring appeared in the region of 1355-1350 cm⁻¹ for compounds **6d-f** and **6j-l**. The medium intensity stretching of C-N single bond containing phthalazine ring appeared in the region of 1236-1230 cm⁻¹, the medium stretching of C-O-C appeared in the region of 1215-1190 cm⁻¹, the medium stretching of nitrogen and nitrogen (-N-N-) containing phthalazine ring appeared in 1096-1085 cm⁻¹ region for the synthesized compounds **6a-l**.

In ¹H NMR spectra, two protons of the primary amine group appeared as a singlet in the region of 8.85-8.40 ppm; fourteen aromatic protons appeared as a multiplet (m) in the region of 8.67-7.23 ppm, one aromatic chiral proton appeared as a singlet (s) in the region of 6.62-6.42 ppm for all twelve compounds. The R₁-substituted methyl protons attached to the quinoline ring resonate in the region of 2.52-2.44 ppm as a singlet (s) for compounds **6b**, **6e**, **6h** and **6k**. R₂-substituted methoxy protons attached to the quinoline ring resonate in the region of 3.86-3.80 ppm as a singlet (s) for compounds **6c**, **6f**, **6i** and **6l**. Methylene protons of R₃-substituted ethyl ester resonate in 4.03-3.95 ppm region as a quartet (q) for **6g** to **6l** and the methyl group of R₃-substituted ethyl ester resonates in 1.08-0.96 ppm region as a triplet (t) for **6g** to **6l**.

In ¹³C NMR spectra, the methylene carbon of R₁-substitution showed a single line in the range of 21.40-21.62 ppm for the compounds **6b**, **6e**, **6h** and **6k** while the methoxy carbon of R₁-substitution showed a single line in the range 55.85-55.94 ppm for compounds **6c**, **6f**, **6i** and **6l**. The methyl and oxymethylene carbon of the R₃-substituted ester showed two signals in the appropriate range of 14.20-14.50 and 63.30-64.01 ppm for compounds **6g-l**. Active methylene (C₁) carbon showed a single line in the range of 58.92-60.20 ppm for compounds **6a-l**. The R₃-substituted carbon showed a single line in the range of 61.11-62.15 and 81.95-82.45 ppm for the compounds **6a-f** and **6g-l**, respectively. A single line for the carbon of R₃-substituted cyanide group appeared in the range

of 116.31-117.26 ppm for compounds **6a-f**, while the ester group as R₃-substitution showed a single line in the range of 164.15-164.62 ppm for compounds **6g-l**. Two carbonyl carbons of phthalazinedione ring showed two lines in the range of 155.90-158.90 ppm for compounds **6a-l**. Phthalazinedione ring, quinoline ring and phenyl ring carbon showed fourteen lines in the range 123.01-160.47 ppm for all the synthesized twelve compounds.

Antiproliferation and EGFR inhibitory: Antiproliferation activity against adenocarcinomic human alveolar basal epithelial A549 cancer cell line and Hep G2 liver cancer cell line and EGFR kinase inhibitory activity for all the prepared compounds having phthalazinedione and quinoline core was carried out. First-generation EGFR tyrosin kinase inhibitor, inhibits the signal transduction between the two EGFR molecules by binding to the ATP binding receptor site of the mutated tyrosine kinase enzyme and terminating the formation of phosphotyrosine residues. From Table-1, it can be seen that among all the synthesized molecules, compounds **6l**, **6h** and **6k** showed the highest EGFR kinase inhibitory activity for IC₅₀, which is 0.90 ± 0.12 μM, 1.10 ± 0.04 μM and 1.01 ± 0.02 μM, respectively compared to the first-generation EGFR tyrosine kinase inhibitor. The antiproliferative activity against the cancer cell line A549 was found to be highest in case of the synthesized compounds **6l**, **6k**, **6c** and **6h** with the IC₅₀ concentration of 0.19 ± 0.16, 0.25 ± 0.09, 0.32 ± 0.03 and 0.58 ± 0.13 μM, respectively compared to the standard erlotinib. Whereas in the case of activity against Hep G2 cancer cell line, only compounds **6b** and **6d** showed the highest activity with the IC₅₀ concentration of 0.21 ± 0.02 and 0.32 ± 0.11 μM with compared to erlotinib.

TABLE-1
INHIBITION OF EGFR KINASE AND ANTIPROLIFERATIVE
ACTIVITY IC₅₀ (μM) OF COMPOUNDS **6a-l**

Compound	EGFR	A549	Hep G2
6a	21.02 ± 0.13	18.45 ± 0.01	15.20 ± 0.02
6b	3.25 ± 0.02	2.23 ± 0.01	0.21 ± 0.02
6c	2.10 ± 0.21	0.32 ± 0.03	8.13 ± 0.06
6d	19.58 ± 0.32	4.34 ± 0.14	0.32 ± 0.11
6e	28.70 ± 0.09	10.03 ± 0.04	4.83 ± 0.15
6f	17.05 ± 0.10	3.10 ± 0.05	1.25 ± 0.08
6g	22.09 ± 0.13	7.16 ± 0.01	7.21 ± 0.13
6h	1.01 ± 0.02	0.58 ± 0.13	3.30 ± 0.05
6i	2.08 ± 0.07	3.16 ± 0.09	2.84 ± 0.12
6j	31.68 ± 0.21	6.30 ± 0.19	2.40 ± 0.04
6k	1.10 ± 0.04	0.25 ± 0.09	7.04 ± 0.05
6l	0.90 ± 0.12	0.19 ± 0.16	2.21 ± 0.16
Erlotinib	0.032 ± 0.002	0.13 ± 0.01	0.12

Antibacterial and *E. coli* FabH inhibitory: Antibacterial activity of the synthesized compounds was carried out against *B. subtilis* and *S. aureus* as Gram positive bacteria and *E. coli* and *P. aeruginosa* as Gram-negative bacteria with kanamycin B and penicillin G as a standard. Against the Gram-positive *B. subtilis* bacteria, none of the synthesized molecules showed any significant activity, whereas for *S. aureus*, compounds **6c**, **6d** and **6i** showed a significant activity compared to penicillin G standard. Compounds **6c** and **6i** showed the highest activity

compared to the standards against *E. coli*, while for *P. aeruginosa*, compounds **6h** and **6j** showed a significant activity when compared to penicillin G. The minimum inhibitory concentration ($\mu\text{g/mL}$) for all the synthesized compounds against the selected strain of bacteria is summarized in Table-2.

Compounds	Minimum inhibitory concentrations ($\mu\text{g/mL}$)			
	Gram-positive		Gram-negative	
	<i>B. subtilis</i> ATCC 6633	<i>S. aureus</i> ATCC 6538	<i>E. coli</i> ATCC 35218	<i>P. aeruginosa</i> ATCC 13525
6a	12.5	>50	>50	>50
6b	3.13	50	6.25	50
6c	25	6.25	3.13	12.5
6d	>50	3.13	12.5	50
6e	>50	25	25	25
6f	25	25	25	25
6g	25	>50	50	25
6h	25	50	50	6.25
6i	6.25	3.13	1.56	12.5
6j	50	25	25	6.25
6k	12.5	12.5	>50	>50
6l	>50	12.5	12.5	12.5
Kanamycin B	0.39	1.56	1.56	3.13
Penicillin G	1.56	6.25	3.13	6.25

E. coli FabH inhibitory activity against the synthesized molecules **6a-l** was also carried out. Compounds **6b**, **6c**, **6f** and **6i** showed potent *E. coli* FabH inhibitory activity. The most potent inhibitory activity with IC_{50} of $3.4 \mu\text{M}$ was exhibited by compound **6i**. This result supported the potent antibacterial activity of compound **6i**. Among other compounds, compound **6c** ($\text{IC}_{50} = 4.1 \mu\text{M}$), **6f** ($\text{IC}_{50} = 5.6 \mu\text{M}$) and **6b** ($\text{IC}_{50} = 9.4 \mu\text{M}$) were found to possess effective *E. coli* FabH inhibitory activity (Table-3).

Compounds	<i>E. coli</i> FabH IC_{50} (μM)	Hemolysis LC_{30}^a (mg/mL)
6a	27.4	> 10
6b	9.4	> 10
6c	4.1	> 10
6d	22.1	> 10
6e	11.8	> 10
6f	5.6	> 10
6g	23.1	> 10
6h	25.6	> 10
6i	3.4	> 10
6j	18.5	> 10
6k	21.8	> 10
6l	20.9	> 10

^aLytic concentration 30%

Molecular docking study

EGFR: To further enhance the knowledge about the potency of the synthesized compounds and assist further SAR studies, molecular docking was used for all synthesized compounds to check their interaction with EGFR (PDB code: 1M17). The process was carried out by simulation of compounds into the ATP binding site in EGFR. The binding energy of all the synthesized compounds is given in Table-4. Compound **6l** was found to be very effectively bound into the active site of EGFR with minimum binding energy $\Delta G_b = -54.0521 \text{ kcal/mol}$. Fig. 1a shows the binding model of compound **6l** and EGFR. In binding mode, compound **6l** was found to be nicely bound to the ATP binding site of EGFR through hydrophobic interaction and the binding was stabilized by two hydrogen bonds one π -H interaction as shown in Fig. 1b. Out of the two hydrogen bonds formed in compound **6l**, one hydrogen bond forms between the oxygen of the $-\text{OCH}_3$ group and the H atom of HIS781 having a distance: of 3.04 \AA while, another H-interaction forms

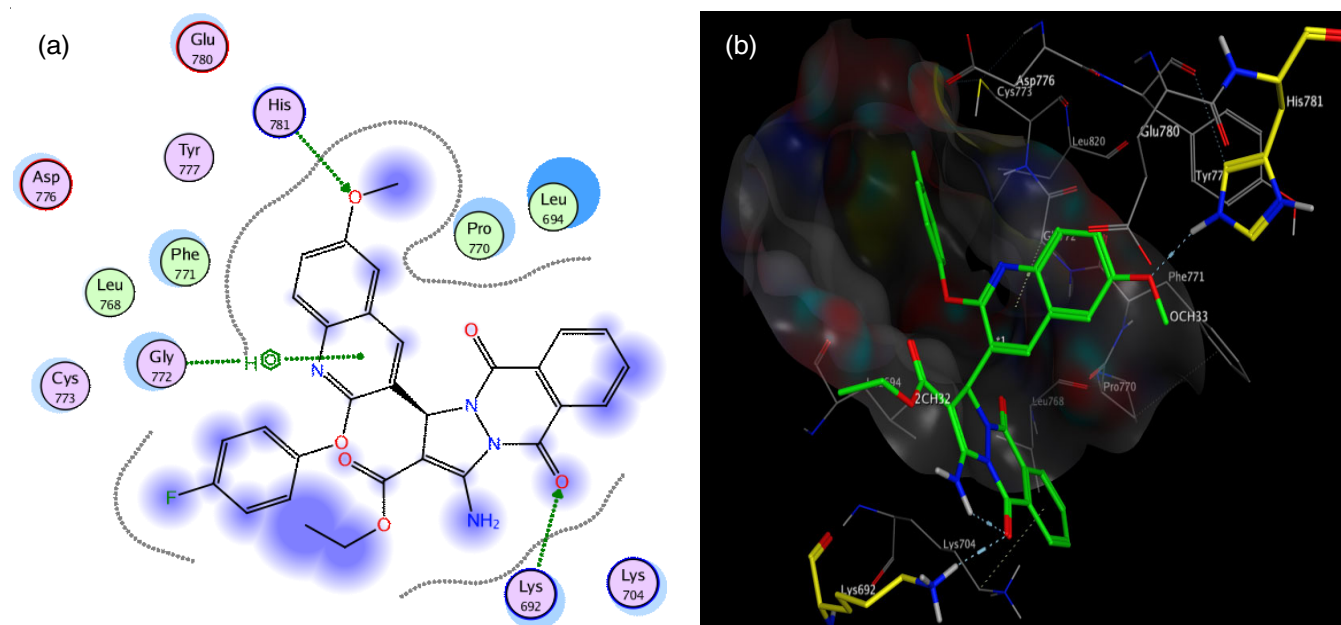


Fig. 1. (a) 2D and (b) 3D binding model of compound **6l** into the active pocket of EGFR

TABLE-4
BINDING ENERGY OF COMPOUNDS **6a-l**
WITH EGFR AND FabH

Compounds	Binding energy (ΔG_b)	
	EGFR	FabH
6a	-43.5756	-38.5282
6b	-50.9727	-41.9521
6c	-52.329	-42.3504
6d	-49.0831	-38.9134
6e	-45.7755	-41.5738
6f	-46.7315	-42.1581
6g	-45.2032	-41.9533
6h	-53.6742	-38.6283
6i	-51.9909	-46.0197
6j	-45.4753	-40.9729
6k	-53.8194	-40.6214
6l	-54.0521	-40.1866

between the O atom of the phthalazine ring and H atom of LYS692 with distance 2.73568 Å. Also, one π -H interaction forms between the benzene ring and GLY772 with a distance of 4.50 Å. The binding interactions obtained by the molecular docking method confirmed that two hydrogen bonds and one π -H interaction are responsible for the effective EGFR inhibitory of compound **6l**.

FabH: Molecular docking of synthesized compounds and *E. coli* FabH was carried out on the binding model based on *E. coli* FabH-CoA complex structure (1HNJ.pdb) for a better understanding of the potency of all synthesized compounds and to help in further SAR studies. A catalytic triad tunnel consisting of Cys-His-Asn is generally present in the FabH active site, which is conserved in various bacteria. This catalytic triad plays a significant role in the regulation of chain elongation and substrate binding. Out of these three, Cys of the catalytic triad of FabH is responsible for breaking the alkyl

chain of CoA, therefore, interactions between Cys and substrate seems to play an important role in substrate binding. Data from a molecular docking study with FabH showed that compound **6i** was effectively bound to the active site of FabH with two hydrogen bonds and one π -H interaction with minimum binding energy $\Delta G_b = -46.0197$ Kcal/mol. The binding energy of all the compounds is given in Table-4. The binding model of compound **6i** and EGFR is shown in Fig. 2a. One H-bond is formed between the H atom of $-NH_2$ group and O atom of GLY152 at a distance of 3.04 Å, while the other H-interaction is formed between the phthalazine ring's O atom and ASN210's hydrogen atom at a distance of 3.11 Å. Also, one π -H interaction forms between the six-membered ring and GLY209 with a distance of 3.86 Å. The binding interactions obtained by the molecular docking method confirmed that two hydrogen bonds and one π -H interaction accounts for the effective FabH inhibitory activity of compound **6i** (Fig. 2b).

Computational studies

Frontier molecular orbitals and DFT: The structural, geometrical parameters and energies of the synthesized compounds (**6a-l**) were calculated by DFT at B3LYP level of theory and def2-SVP basis set with the help of ORCA computational chemistry tool [39]. Structures of all the synthesized twelve compounds were also optimized at B3LYP functional level and def2-SVP and the obtained structure were then checked for their global minimum energy, where no imaginary frequency was found. The twist angle between the plane of phthalazine ring and the plane of phenyl ring linked with nucleus with ether group is observed as (θ_1) and the twist angle between the plane of phenyl ring linked with nucleus with ether group and the plane of quinoline is observed as (θ_2).

As electronic properties are mainly dependent on the distribution of charge on the individual atoms as well as the

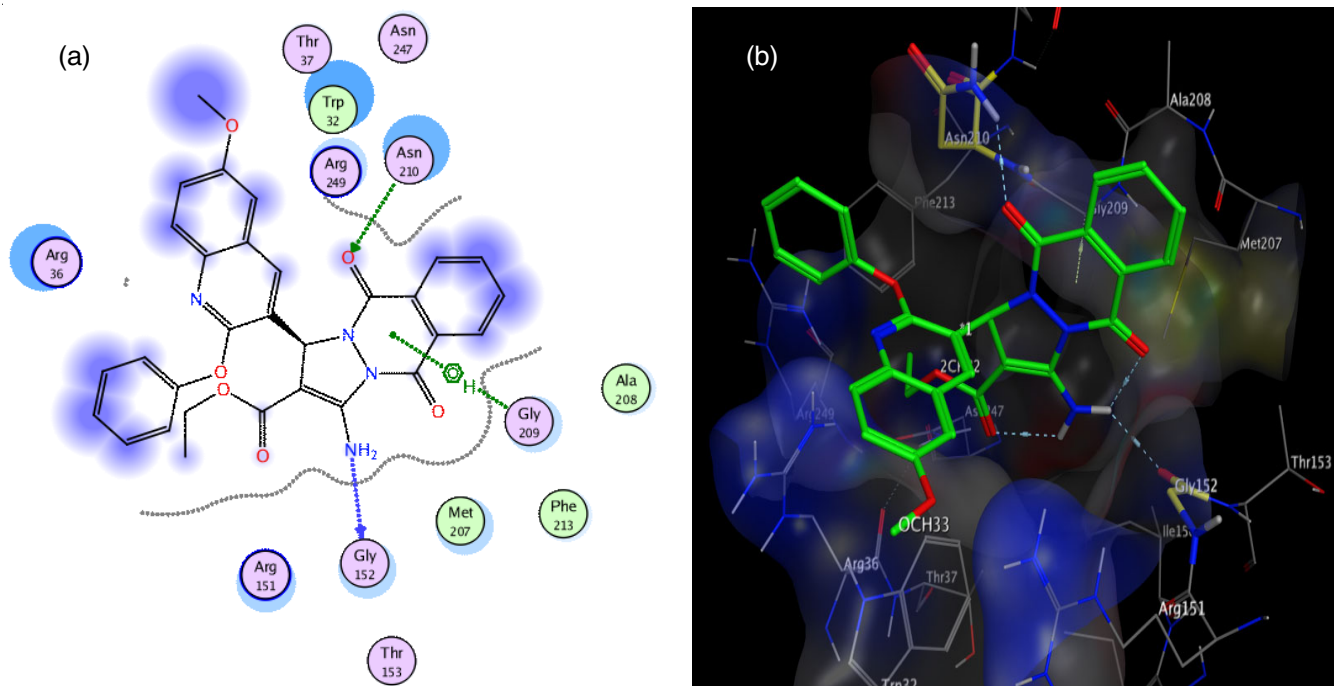


Fig. 2. (a) 2D and (b) 3D binding model of compound **6i** into the active site of FabH

molecular orbitals, the UV-visible properties of the molecules can also be predicted depending, on the solvent system. It is known that, smaller the value of HOMO-LUMO energy gap ΔE , greater will be the reactivity of the molecule [41], also this energy gap ΔE of HOMO-LUMO is associated with the stability and reactivity of the compound. The energy gap ΔE values obtained from the DFT calculations varied between 5.398 eV and 5.642 eV for compound **6a-c**, 5.501 eV and 5.651 eV for compound **6d-f**, 5.591 eV and 5.729 eV for compound **6g-i**, 5.569 eV and 5.723 eV for compound **6j-l**.

From Figs. 3-6, representing the isoidentity surface plot of HOMO-LUMO, it can be seen that there is delocalization of orbital and low number of nodal planes, hence there is strong orbital overlap. As all the synthesized compound have same nucleus and differs only at the substitution at three positions, this variation at the substitution also affects the HOMO-LUMO energy gap ΔE . From the energy gap values of HOMO-LUMO (Table-5), it shows that molecules having $-\text{OCH}_3$ at R_1 substitution position shows higher energy gap value, compared to the other molecules, which differ at only R_1 substitution except molecule **6a**. From the basic relationship between the energy gap and reactivity, it suggests that these compounds must be less reactive. Energy gap ΔE is also related with the softness and hardness η of the molecule, where molecules with high HOMO-LUMO gap are said to be hard and molecules with small HOMO-LUMO gap are said to be soft, the values of these hardness and softness is given in Table-5. It is obvious that molecules with $-\text{OCH}_3$ at R_1 for each group of substitution, are hard molecules where the values of η varies from 2.788 (compound **6c**) to 2.864 (compound **6i**), whereas for the soft molecules in each substitution group of molecules, the values of η varies from 2.699 (compound **6a**) to 2.795 (compound **6g**). Like hardness and softness of molecules, there are other

such quantum chemical parameters, which are dependent on the energy gap values of HOMO and LUMO. From these values given in Table-5, compound **6a** is the absolute soft, whereas compounds **6i** and **6h** are the absolute hard compound, yet from the data of inhibition of EGFR kinase and *E. coli* FabH inhibitory activity, compounds **6l** and **6i** were found most active among the presented synthesized molecules, thus evaluation of structural activity relationship of any molecule on the basis of its HOMO-LUMO energy gap only is not sufficient to explain its reactivity.

Molecular docking: From the inhibition of EGFR kinase and antiproliferative activity data obtained for molecules **6a-l**, it is found that molecule **6l** have the highest activity against EGFR with 0.90 ± 0.12 at IC_{50} (μM), while molecule **6j** showed lowest activity with IC_{50} (μM) value of 31.68 ± 0.21 . As these two compounds differ from each other at the R_1 substitution group, the optimized geometry suggests that there is a decrease in the twist angle θ_1 by 2.79° and decrease in the twist angle θ_1 by 4.52° . Due to the presence of methoxy group on quinoline ring, it changes the position of quinoline ring in the space and enhances the chances of hydrogen bond formation with the HIS781 in plane 1, while the second hydrogen bond form at the phthalazine ring's oxygen atom and LYS692 in plane 3 (Figs. 7-10), these two hydrogen bonds are perpendicular to each other resulting in the closed pack interaction and hence it has lowest binding energy ΔG_b , while the absence of hydrogen bond at the quinoline end in molecule **6j**, does not result in such closed pack interaction with the protein as it has only hydrogen atom at R_1 substituent position.

E. coli FabH inhibitory activity data for all the synthesized compounds (**6a-l**) suggests that compound **6i** has the highest activity against *E. coli*, while compound **6a** exhibited the lowest activity. In molecule **6i**, phthalazine ring and phenyl ring are

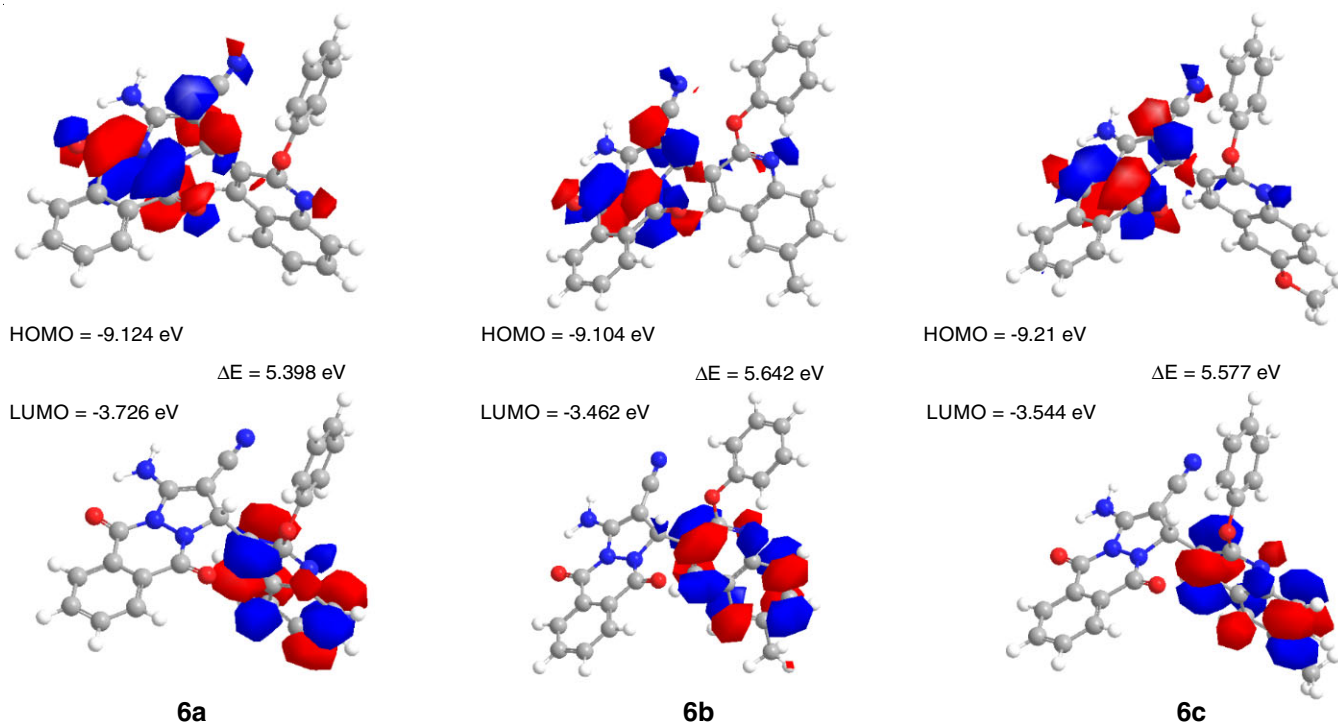
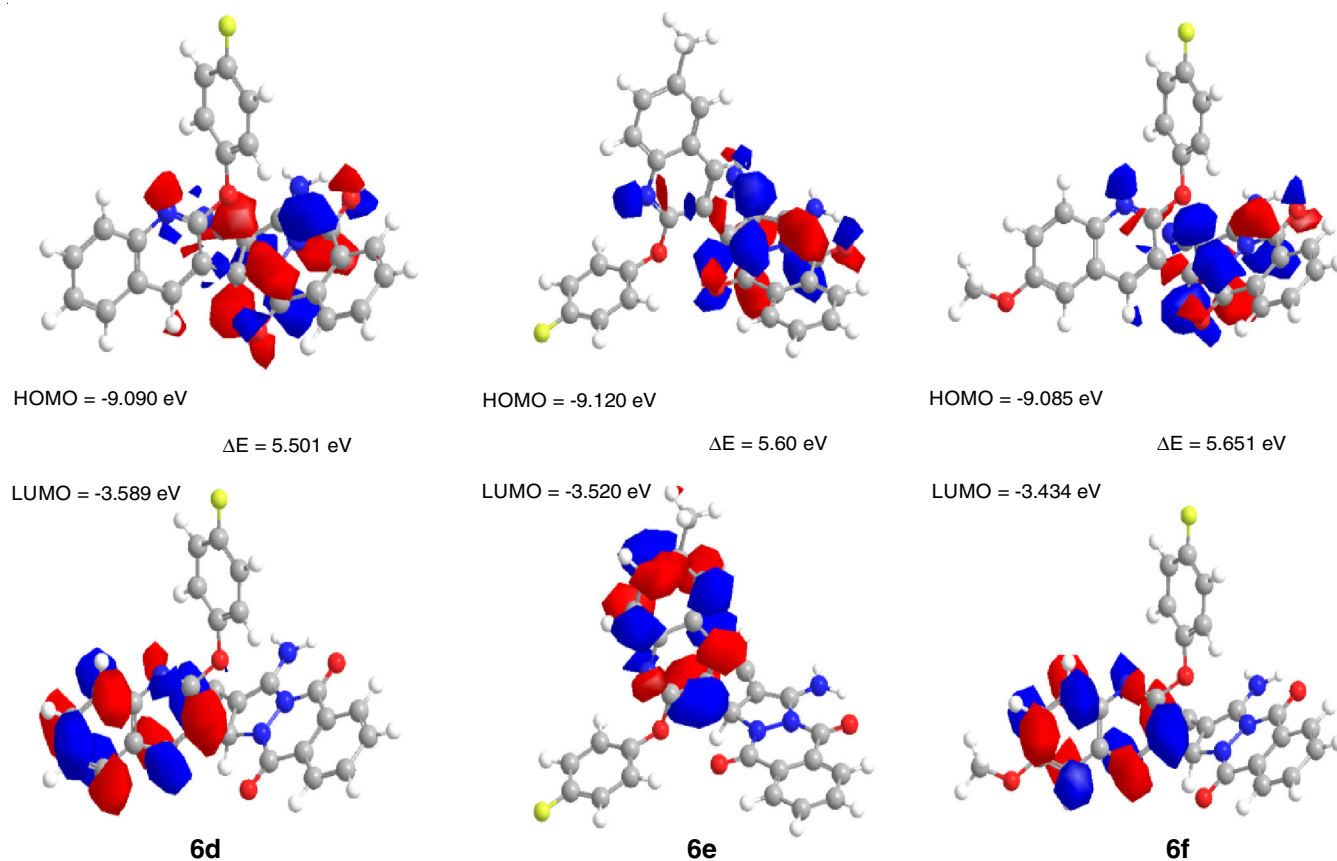
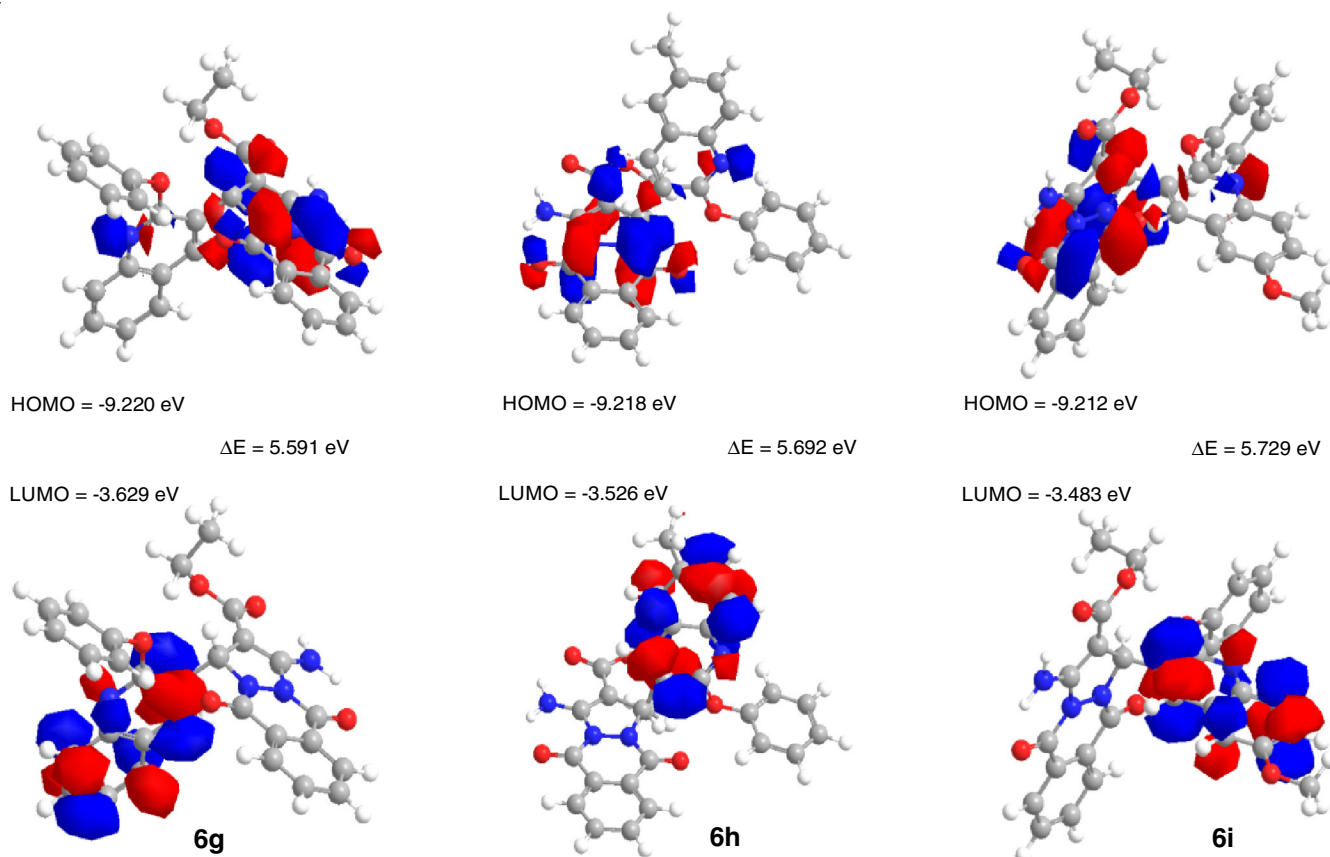


Fig. 3. Frontier molecular orbitals diagram of **6a-c**

Fig. 4. Frontier molecular orbitals diagram of **6d-f**Fig. 5. Frontier molecular orbitals diagram of **6g-i**

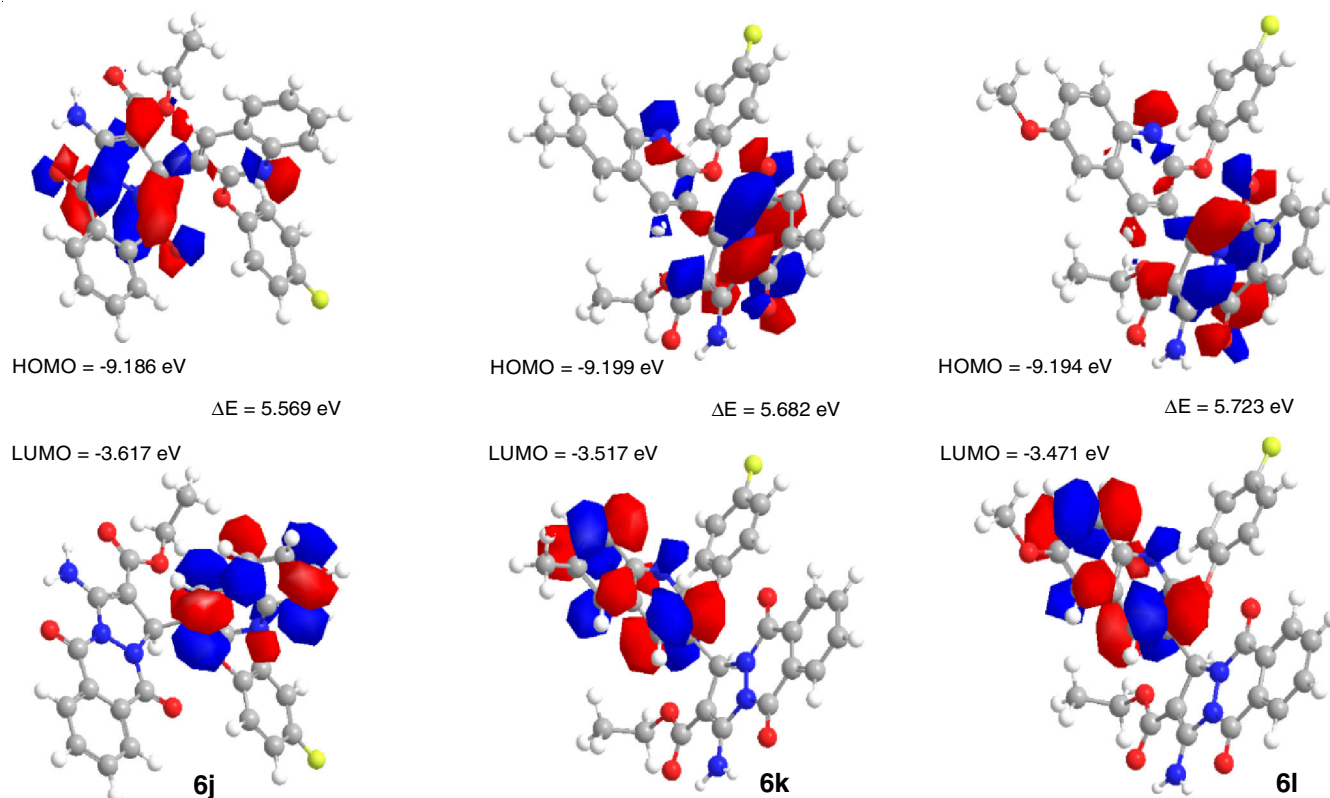
Fig. 6. Frontier molecular orbitals diagram of **6j-l**

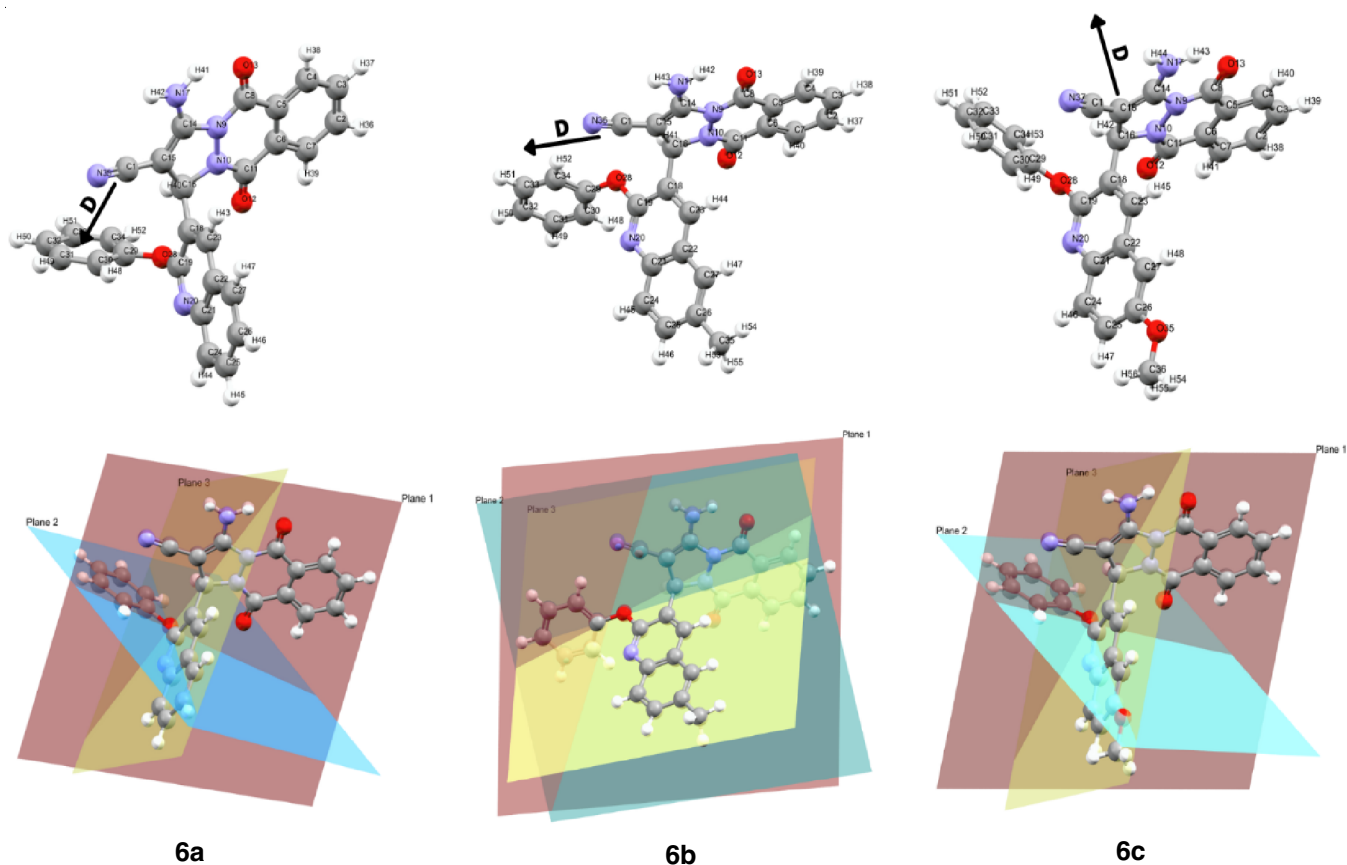
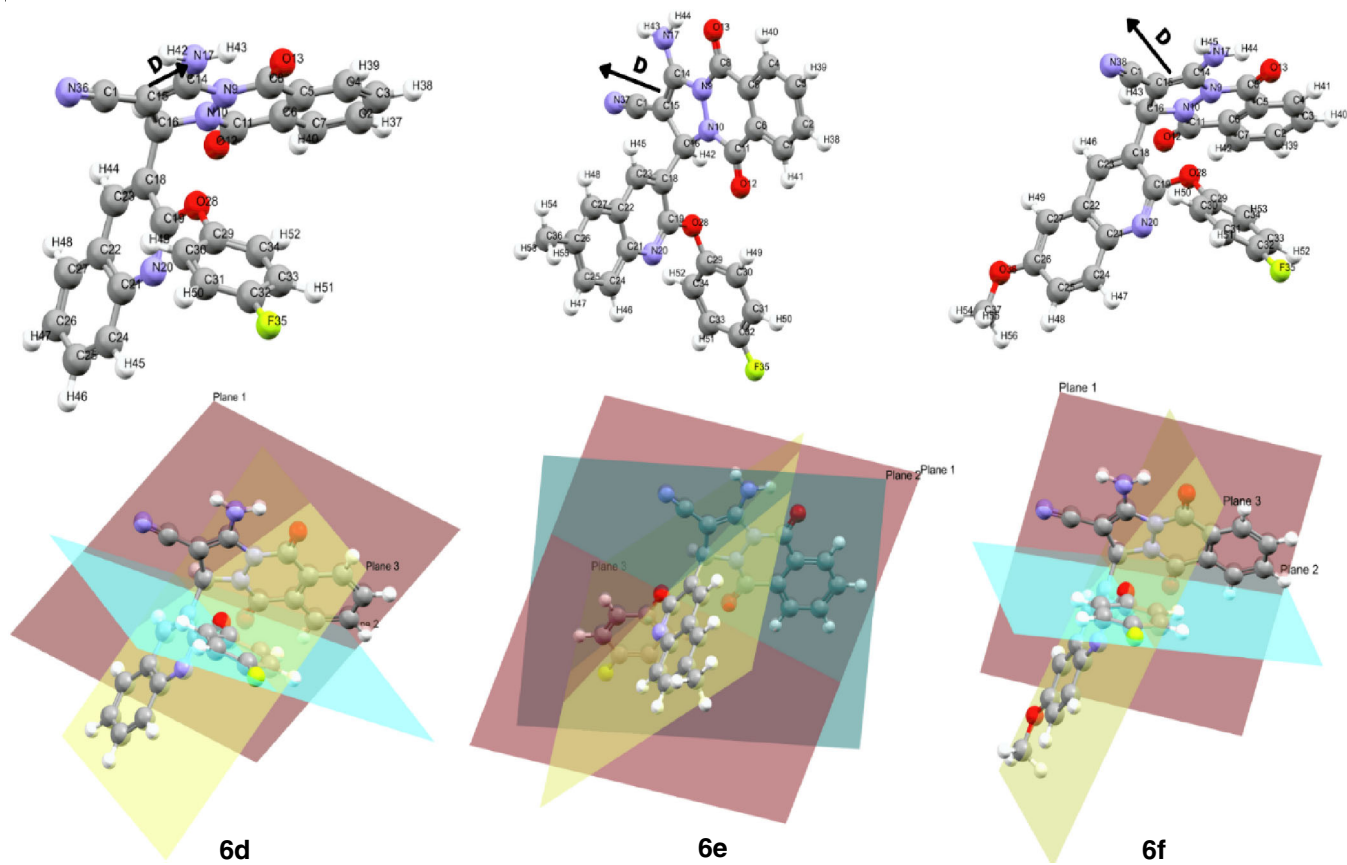
TABLE-5
CALCULATED CHARGES ON DONATING SITES AND ENERGY VALUES HOMO, LUMO, ENERGY GAP ΔE/eV, DIPOLE MOMENTS, ENERGIES, TWIST ANGLE (θ), HARDNESS (η), GLOBAL SOFTNESS (S), ELECTRO NEGATIVITY (χ), ABSOLUTE SOFTNESS (σ), CHEMICAL POTENTIAL (π), GLOBAL ELECTROPHILICITY (ω) AND ADDITIONAL ELECTRONIC CHARGE (ΔN_{max}) OF THE STUDIED COMPOUNDS **6a-l** BY USING DFT CALCULATIONS

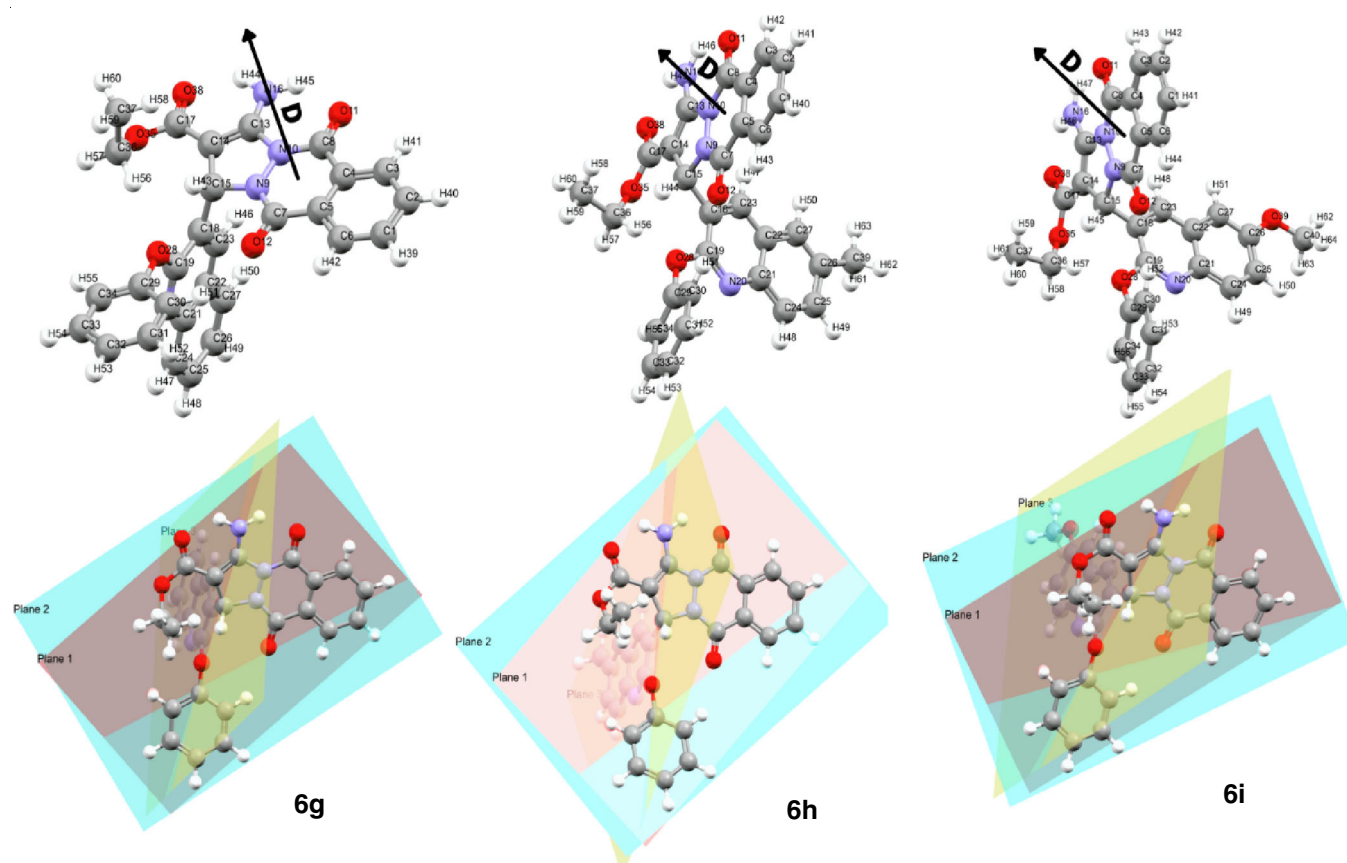
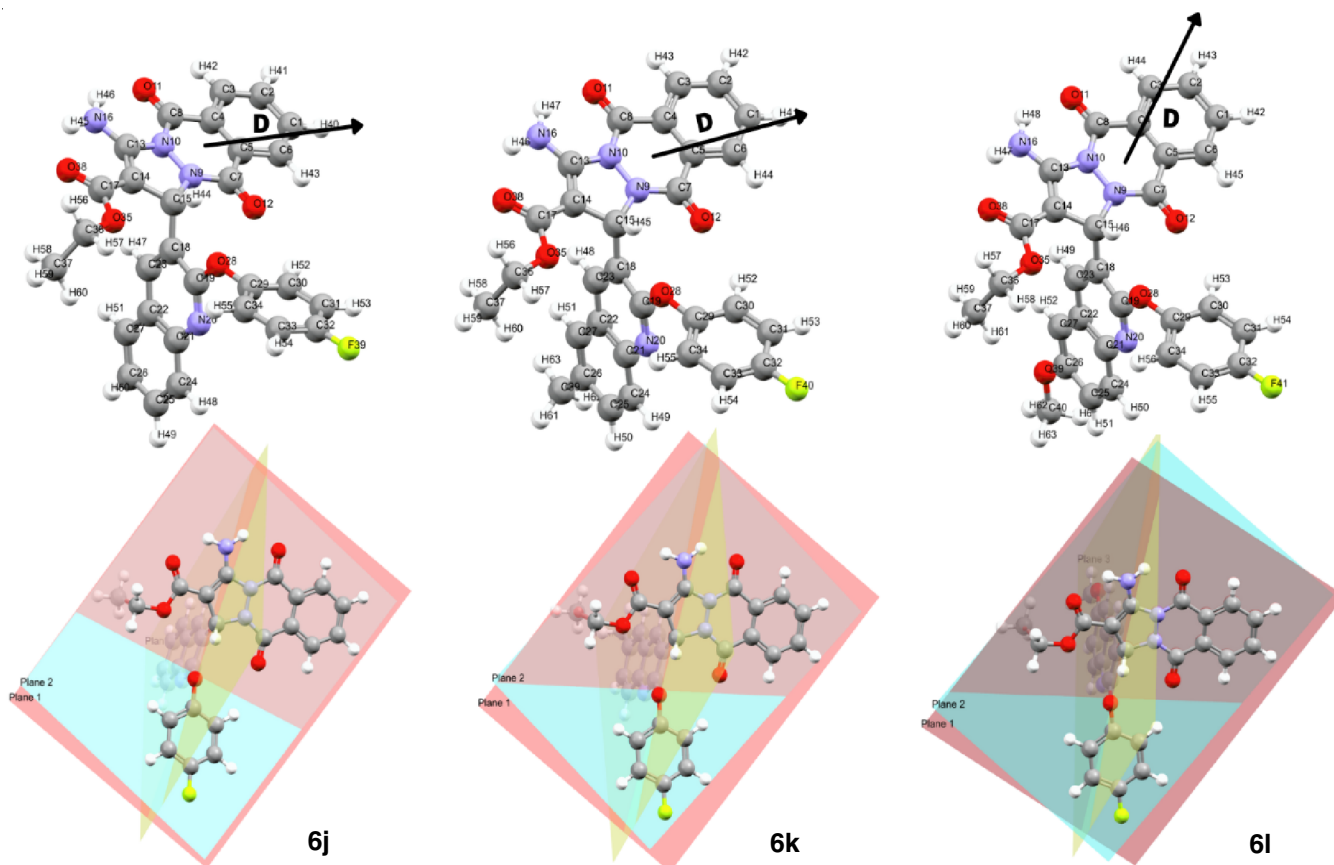
Parameters	6a	6b	6c	6d	6e	6f	6g	6h	6i	6j	6k	6l
E _{HOMO} (eV)	-9.124	-9.104	-9.121	-9.090	-9.120	-9.085	-9.220	-9.218	-9.212	-9.186	-9.199	-9.194
E _{LUMO} (eV)	-3.726	-3.462	-3.544	-3.589	-3.520	-3.434	-3.629	-3.526	-3.483	-3.617	-3.517	-3.471
I = -E _{HOMO}	9.124	9.104	9.121	9.090	9.120	9.085	9.220	9.218	9.212	9.186	9.199	9.194
A = -E _{LUMO}	3.726	3.462	3.544	3.589	3.520	3.434	3.629	3.526	3.483	3.617	3.517	3.471
ΔE = I - A (eV)	5.398	5.642	5.577	5.501	5.600	5.651	5.591	5.692	5.729	5.569	5.682	5.723
Dipole moment (Debye)	6.26	6.34	5.90	4.33	7.08	3.88	4.33	4.30	4.59	3.74	3.97	3.65
Energy (a.u)	-1536.54	-1575.81	-1650.91	-1635.69	-1697.93	-1750.05	-1711.27	-1750.53	-1825.65	-1810.42	-1849.68	-1924.79
Twist angle (θ)	θ ₁	76.87	16.59	77.10	57.77	12.79	57.42	10.77	10.37	10.11	15.75	12.90
	θ ₂	86.43	67.55	87.31	71.22	84.04	69.77	78.98	79.40	81.04	89.68	85.16
η = (I - A)/2	2.699	2.821	2.788	2.750	2.800	2.825	2.795	2.846	2.864	2.784	2.841	2.861
χ = (I + A)/2	6.425	6.273	6.332	6.339	6.320	6.259	6.424	6.372	6.321	6.401	6.358	6.332
σ = 1/η	0.371	0.354	0.359	0.364	0.357	0.354	0.358	0.351	0.349	0.359	0.352	0.350
S = 1/2η	0.185	0.177	0.179	0.182	0.179	0.177	0.179	0.176	0.175	0.180	0.176	0.175
π = -χ	-6.425	-6.273	-6.332	-6.339	-6.320	-6.259	-6.424	-6.372	-6.321	-6.401	-6.358	-6.332
ω = (π) ² /2η	7.647	6.975	7.190	7.306	7.133	6.934	7.382	7.133	6.975	7.359	7.114	7.007
ΔN _{max} = χ/η	2.381	2.224	2.271	2.305	2.257	2.216	2.298	2.239	2.207	2.299	2.238	2.213

in about same plane, maintaining planarity in molecule, due to which ASN210 hydrogen bonding is favourable, while in molecule **6a**, phthalazine ring and phenyl ring are in different plane having twist angle of 76.87°. The van der Waal's radii of quinoline ring hinders the interaction between phthalazine ring's oxygen and ASN210, reducing its activity. Figs. 7 and 9 shows the twist angle θ₁ of molecules **6a** and **6i**, which are 76.87° and 10.11° respectively, with a difference of 66.76°, which supports the above conclusion.

Conclusion

In summary, 2-aryloxyquinoline moiety of a novel series of 1*H*-pyrazolo[1,2-*b*]phthalazine-5,10-diones has been produced in high yield using base catalyzed one-pot multi-component synthesis. This synthetic approach provides an easy way to allow the assimilation of two promising bioactive nuclei in a single scaffold. The most of the synthesised compounds displayed strong antibacterial and anticancer activities, as determined by an indepth analysis of their biological activities.

Fig. 7. Twist angle θ and dipole moment of 6a-cFig. 8. Twist angle θ and dipole moment of 6d-f

Fig. 9. Twist angle θ and dipole moment of **6g-i**Fig. 10. Twist angle θ and dipole moment of **6j-l**

The most effective members of the series in terms of inhibitory activity were compounds **6h**, **6k** and **6l** against EGFR and compounds **6c**, **6f** and **6i** against FabH. Therefore, it is worth to mention that 1*H*-pyrazolo[1,2-*b*]phthalazine-5,10-diones having 2-aryloxyquinoline moiety has emerged as a key area in the development of antibiotics and cancer treatments. All these synthesized compounds were optimized with DFT to obtain their arrangement in space to evaluate plane angle on the basis of the substitutions, these plane angles were then related with their activity against EGFR and FabH in terms of binding efficiency, antibacterial as well as anticancer activities.

ACKNOWLEDGEMENTS

The authors are thankful to Shri Maneklal M. Patel Institute of Sciences and Research, Kadi Sarva Vishwavidhyalaya for providing the infrastructure and laboratory facility.

CONFLICT OF INTEREST

The authors declare that there is no conflict of interests regarding the publication of this article.

REFERENCES

- N. Kerru, L. Gummidi, S. Maddila, K.K. Gangu and S.B. Jonnalagadda, *Molecules*, **25**, 1909 (2020); <https://doi.org/10.3390/molecules25081909>
- J. Jampilek, *Molecules*, **24**, 3839 (2019); <https://doi.org/10.3390/molecules24213839>
- B.S. Matada, R. Pattanashettar and N.G. Yernale, *Bioorg. Med. Chem.*, **32**, 115973 (2021); <https://doi.org/10.1016/j.bmc.2020.115973>
- S. Jain, V. Chandra, P. Kumar Jain, K. Pathak, D. Pathak and A. Vaidya, *Arab. J. Chem.*, **12**, 4920 (2019); <https://doi.org/10.1016/j.arabj.2016.10.009>
- E.J. Meuillet and E.G. Bremer, *Pediatr. Neurosurg.*, **29**, 1 (1998); <https://doi.org/10.1159/00028677>
- J.Y. Lee, K.W. Jeong, S. Shin, J.U. Lee and Y. Kim, *Bioorg. Med. Chem.*, **17**, 5408 (2009); <https://doi.org/10.1016/j.bmc.2009.06.059>
- C.Y. Lai and J.E. Cronan, *J. Biol. Chem.*, **278**, 51494 (2003); <https://doi.org/10.1074/jbc.M308638200>
- M. Tateishi and T. Ishida, *Cancer Res.*, **50**, 7077 (1990).
- S.W. White, J. Zheng, Y.M. Zhang and C.O. Rock, *Annu. Rev. Biochem.*, **74**, 791 (2005); <https://doi.org/10.1146/annurev.biochem.74.082803.133524>
- K.S. Kolibaba and B.J. Druker, *Biochim. Biophys. Acta*, **1333**, F217 (1997); [https://doi.org/10.1016/s0304-419x\(97\)00022-x](https://doi.org/10.1016/s0304-419x(97)00022-x)
- M.S. Abdelbaset, M. Abdel-Aziz, M. Ramadan, M.H. Abdelrahman, S.N. Abbas Bukhari, T.F.S. Ali and G.E.-D.A. Abuo-Rahma, *Bioorg. Med. Chem.*, **27**, 1076 (2019); <https://doi.org/10.1016/j.bmc.2019.02.012>
- M.J. Akhtar, M. Ahamed, H.A. Alhadlaq, S.A. Alrokayan and S. Kumar, *Clin. Chim. Acta*, **436**, 78 (2014); <https://doi.org/10.1016/j.cca.2014.05.004>
- L. Chen, W. Fu, L. Zheng, Z. Liu and G. Liang, *J. Med. Chem.*, **61**, 4290 (2018); <https://doi.org/10.1021/acs.jmedchem.7b01310>
- M. Singh and H.R. Jadhav, *Drug Discov. Today*, **23**, 745 (2018); <https://doi.org/10.1016/j.drudis.2017.10.004>
- H.H. Jardosh and M.P. Patel, *Eur. J. Med. Chem.*, **65**, 348 (2013); <https://doi.org/10.1016/j.ejmech.2013.05.003>
- C.B. Sangani, J.A. Makawana, Y.-T. Duan, Y. Yin, S.B. Teraiya, N.J. Thumar and H.-L. Zhu, *Bioorg. Med. Chem. Lett.*, **24**, 4472 (2014); <https://doi.org/10.1016/j.bmcl.2014.07.094>
- Y. Jia, C.H. Yun, E. Park, D. Ercan, M. Manuia, J. Juarez, C. Xu, K. Rhee, T. Chen, H. Zhang, S. Palakurthi, J. Jang, G. Lelais, M. DiDonato, B. Bursulaya, P.-Y. Michellys, R. Epple, T.H. Marsilje, M. McNeill, W. Lu, J. Harris, S. Bender, K.-K. Wong, P.A. Jänne and M.J. Eck, *Nature*, **534**, 129 (2016); <https://doi.org/10.1038/nature17960>
- J.R. Li, D.D. Li, R.R. Wang, J. Sun, J.-J. Dong, Q.-R. Du, F. Fang, W.-M. Zhang and H.-L. Zhu, *Eur. J. Med. Chem.*, **75**, 438 (2014); <https://doi.org/10.1016/j.ejmech.2013.11.020>
- A.C. Price, K.H. Choi, R.J. Heath, Z. Li, S.W. White and C.O. Rock, *J. Biol. Chem.*, **276**, 6551 (2001); <https://doi.org/10.1074/jbc.M007101200>
- M. Leeb, *Nature*, **431**, 892 (2004); <https://doi.org/10.1038/431892a>
- S.S. Khandekar, D.R. Gentry, G.S. Van Aller, P. Warren, H. Xiang, C. Silverman, M.L. Doyle, P.A. Chambers, A.K. Konstantinidis, M. Brandt, R.A. Daines and J.T. Lonsdale, *J. Biol. Chem.*, **276**, 30024 (2001); <https://doi.org/10.1074/jbc.M101769200>
- X. Qiu, C.A. Janson, W.W. Smith, M. Head, J. Lonsdale and A.K. Konstantinidis, *J. Mol. Biol.*, **307**, 341 (2001); <https://doi.org/10.1006/jmbi.2000.4457>
- S.S. Khandekar, R.A. Daines and J.T. Lonsdale, *Curr. Protein Pept. Sci.*, **4**, 21 (2003); <https://doi.org/10.2174/1389203033380377>
- R.J. Heath and C.O. Rock, *J. Biol. Chem.*, **271**, 10996 (1996); <https://doi.org/10.1074/jbc.271.18.10996>
- Z. Nie, C. Perretta, J. Lu, Y. Su, S. Margosiak, K.S. Gajiwala, J. Cortez, V. Nikulin, K.M. Yager, K. Appelt and S. Chu, *J. Med. Chem.*, **48**, 1596 (2005); <https://doi.org/10.1021/jm049141s>
- J. Wang, S. Kodali, S.H. Lee, A. Galgoci, R. Painter, K. Dorso, F. Racine, M. Motyl, L. Hernandez, E. Tinney, S.L. Colletti, K. Herath, R. Cummings, O. Salazar, I. González, A. Basilio, F. Vicente, O. Genilloud, F. Pelaez, H. Jayasuriya, K. Young, D.F. Cully and S.B. Singh, *Proc. Natl. Acad. Sci. USA*, **104**, 7612 (2007); <https://doi.org/10.1073/pnas.0700746104>
- R.J. Heath and C.O. Rock, *Curr. Opin. Investig. Drugs*, **5**, 146 (2004).
- D.M. Shin, J.Y. Ro, W.K. Hong and W.N. Hittelamn, *Cancer Res.*, **54**, 3153 (1994).
- R.P. Jain and J.C. Vederas, *Bioorg. Med. Chem. Lett.*, **14**, 3655 (2004); <https://doi.org/10.1016/j.bmcl.2004.05.021>
- A. Kumar, M.K. Gupta and M. Kumar, *Green Chem.*, **14**, 290 (2012); <https://doi.org/10.1039/C1GC16297G>
- R. Ghahremanzadeh, G.I. Shakibaei and A. Bazgir, *Synlett*, **8**, 1129 (2008); <https://doi.org/10.1055/s-2008-1072716>
- D.S. Raghuvanshi and K.N. Singh, *Tetrahedron Lett.*, **52**, 5702 (2011); <https://doi.org/10.1016/j.tetlet.2011.08.111>
- C.B. Sangani, H.H. Jardosh, M.P. Patel and R.G. Patel, *Med. Chem. Res.*, **22**, 3035 (2013); <https://doi.org/10.1007/s00044-012-0322-5>
- H.G. Kathrotiya and M.P. Patel, *Eur. J. Med. Chem.*, **63**, 675 (2013); <https://doi.org/10.1016/j.ejmech.2013.03.017>
- J.A. Makawana, D.C. Mungra, M.P. Patel and R.G. Patel, *Bioorg. Med. Chem. Lett.*, **21**, 6166 (2011); <https://doi.org/10.1016/j.bmcl.2011.07.123>
- J.A. Makawana, C.B. Sangani, L. Lin and H.-L. Zhu, *Bioorg. Med. Chem. Lett.*, **24**, 1734 (2014); <https://doi.org/10.1016/j.bmcl.2014.02.041>
- C.B. Sangani, J.A. Makawana, X. Zhang and S.B. Teraiya, *Bioorg. Med. Chem. Lett.*, **76**, 549 (2014); <https://doi.org/10.1016/j.ejmech.2014.01.018>
- H.R. Tsou, N. Mamuya, B.D. Johnson, M.F. Reich, B.C. Gruber, F. Ye, R. Nilakantan, R. Shen, C. Discafani, R. DeBlanc, R. Davis, F.E. Koehn, L.M. Greenberger, Y.F. Wang and A. Wissner, *J. Med. Chem.*, **44**, 2719 (2001); <https://doi.org/10.1021/jm0005555>
- F. Neese, *Wiley Interdiscip. Rev. Comput. Mol. Sci.*, **8**, e1327 (2017); <https://doi.org/10.1002/wcms.1327>
- R. Huey, G.M. Morris, A.J. Olson and D.S. Goodsell, *J. Comput. Chem.*, **28**, 1145 (2007); <https://doi.org/10.1002/jcc.20634>
- R. Kurtaran, S. Odabasioglu, A. Azizoglu, H. Kara and O. Atakol, *Polyhedron*, **26**, 5069 (2007); <https://doi.org/10.1016/j.poly.2007.07.021>